Inorg. Chem. **2007**, *46*, 6002–6010

Polyoxomolybdenum(V/VI)–Sulfite Compounds: Synthesis, Structural, and Physical Studies

Nikolaos I. Kapakoglou,[†] Betzios I. Panagiotis,[†] Spiros E. Kazianis,[‡] Constantine E. Kosmidis,[‡] Chryssoula Drouza,[§] Manolis J. Manos,*[,∥] Michael P. Sigalas,*[,⊥] Anastasios D. Keramidas,*[,§] and Themistoklis A. Kabanos*[,†]

Section of Inorganic and Analytical Chemistry, Department of Chemistry, University of Ioannina, 45110, Greece, Department of Physics, University of Ioannina, 45110, Greece, Department of Chemistry, University of Cyprus, 1678, Nicosia, Cyprus, Department of Chemistry, Michigan State University, East Lansing, Michigan 48824, and Department of Chemistry, Laboratory of Applied Quantum Chemistry, Aristotle University of Thessaloniki, 54124 Thessaloniki, Greece

Received March 9, 2007

Reaction of $Na_2Mo^{VI}O_4 \cdot 2H_2O$ with $(NH_4)_2SO_3$ in the mixed-solvent system H_2O/CH_3CN (pH = 5) resulted in the formation of the tetranuclear cluster $(NH_4)_4[Mo_4^{VI}SO_{16}] \cdot H_2O$ (**1**), while the same reaction in acidic aqueous solution (pH = 5) yielded $(NH_4)_4[Mo_5^{VI}S_2O_{21}] \cdot 3H_2O$ (**2**). Compound $\{(H_2bipy)_2[Mo_5^{VI}S_2O_{21}] \cdot H_2O\}_x$ (**3**) was obtained from the reaction of aqueous acidic solution of $Na_2Mo^{VI}O_4 \cdot 2H_2O$ with $(NH_4)_2SO_3$ (pH = 2.5) and 4,4′-bipyridine (4,4′-bipy). The mixed metal/sulfite species $(NH_4)_7[Co^{III}(Mo_2^{V}O_4)(NH_3)(SO_3)_6] \cdot 4H_2O$ (**4**) was synthesized by reacting $Na_2Mo^{VI}O_4 \cdot 2H_2O$ with $CoCl_2 \cdot 6H_2O$ and $(NH_4)_2SO_3$ with precise control of pH (5.3) through a redox reaction. The X-ray crystal structures of compounds **1**, **2**, and **4** were determined. The structure of compound **1** consists of a ring of four alternately face- and edge-sharing $Mo^{VI}O_6$ octahedra capped by the trigonal pyramidal sulfite anion, while at the base of the Mo_4 ring is an oxo group which is asymmetrically shared by all four molybdenum atoms. Compound **3** is based on the Strandberg-type heteropolyion $[Mo_5^{VI}S_2O_{21}]^{4-}$, and these coordinatively saturated clusters are joined by diprotonated 4,4′-H_2bipy^{2+} through strong hydrogen bonds. Compound **3** crystallizes in the chiral space group *C*2. The structure of compound **4** consists of a novel trinuclear $[Co^{III}Mo_2^{V}SO_3^{2-}]$ cluster. The chiral compound **3** exhibits nonlinear optical (NLO) and photoluminescence properties. The assignment of the sulfite bands in the IR spectrum of **4** has been carried out by density functional calculations. The cobalt in **4** is a d^6 octahedral low-spin metal atom as it was evidenced by magnetic susceptibility measurements, cw EPR, BVS, and DFT calculations. The IR and solid-state UV–vis spectra as well as the thermogravimetric analyses of compounds **1**–**4** are also reported.

Introduction

The great interest in polyoxometalates (POMs) reflects the diverse nature of this family of inorganic clusters, which exhibit a wide variety of compositions and structural versatility,[1] as well as important optical,[1] catalytic,[1] and magnetic[2] properties. Most attention has been given to heteropolyanions, containing tetrahedral phosphate groups,[3] because of the fascinating electronic and structural properties of polyoxomolybdenum and polyoxovanadium phosphates.[3] In marked contrast, there are only a few examples of heteropolyoxometalates (HPOMs) incorporating the nontetra-

* To whom correspondence should be addressed. E-mail: tkampano@cc.uoi.gr (T.A.K.). Phone: (+30)26510-98415 (T.A.K.). Fax: (+30)26510-44831 (T.A.K.).
[†] Department of Chemistry, University of Ioannina.
[‡] Department of Physics, University of Ioannina.
[§] University of Cyprus.
[∥] Michigan State University.
[⊥] Aristotle University of Thessaloniki.

(1) (a) Pope, M. T. *Heteropoly and Isopoly Oxometalates*; Springer-Verlag: New York, 1983. (b) Pope, M. T., Müller, A., Eds. *Polyoxometalates: From Platonic Solids to Anti-Retroviral Activity*; Kluwer Academic Publishers: Dordrecht, The Netherlands, 1994. (c) Hill, C. L., Guest Editor. *Chem. Rev.* **1998**, *98*, 8. (d) Hussain, F.; Reicke, M.; Kortz, U. *Angew. Chem., Int. Ed.* **2005**, *44*, 3773. (e) Hussain, F.; Kortz, U.; Keita, B.; Nadjo, L.; Pope, M. T. *Inorg. Chem.* **2006**, *45*, 761. (f) Laurencin, D.; Villanneau, R.; Herson, P.; Thouvenot, R.; Jeannin, Y.; Proust, A. *Chem. Commun.* **2005**, 5524. (g) Long, D. L.; Kögerler, P.; Parenty, A. D. C.; Fielden, J.; Cronin, L. *Angew. Chem., Int. Ed.* **2006**, *45*, in press. (h) Zimmermann, M.; Belai, N.; Butcher, R. J.; Pope, M. T.; Chubarova, E. V.; Dickman, M. H.; Kortz, U. *Inorg. Chem.* **2007**, *46*, 1737.

10.1021/ic700460b CCC: $37.00
Published on Web 06/26/2007

hedral sulfite anion.[4] The sulfite anion has C_{3v} symmetry and contains a nonbonding but stereochemically active pair of electrons, and thus, its noncentrosymmetric metal complexes may potentially display nonlinear optical properties (NLO), which until now were observed in the metal−selenites/iodates, etc.[5] In addition, the enzyme sulfite oxidase, which is associated with the in vivo oxidation of SO_3^{2-} to SO_4^{2-}, contains a molybdenum atom at its active center,[6] and thus, access to HPOM-based sulfite architectures is an attractive goal. Furthermore, the use of the 3-connected sulfite anion as basic structural unit for the construction of open-framework materials is particularly desirable, since the presence of 3-connected building blocks has been recognized to contribute to large pore sizes and low framework density.[7] First attempts to such a direction for the sulfite anion appeared very recently in the literature.[4f,8]

Being successful in the synthesis of molybdenum−sulfite clusters,[4b] we decided to introduce cobalt in the Mo^{VI}/SO_3^{2-} system, since the Co^{III}/SO_3^{2-} species may be interesting materials from the standpoint of their applications to the chemical and photochemical oxidation of sulfite.[9] The organic ligand 4,4′-bipyridine (4,4′-bipy) was also introduced into Mo^{VI}/SO_3^{2-} system, because hybrid frameworks[10] are an extremely interesting class of compounds, since they combine the unique properties of the metal fragment with those of organic groups. We report the synthesis and structural and physicochemical properties of the heteropolyoxomolybdenum(V/VI)−sulfite clusters $(NH_4)_4[(cis\text{-}Mo^{VI}O_2)_4(\mu_4\text{-}O)(\mu_2\text{-}O)_4(\mu_4\text{-}SO_3)]\cdot H_2O$ (**1**), $(NH_4)_4[(cis\text{-}Mo^{VI}O_2)_5(\mu_2\text{-}O)_5(\mu_5\text{-}SO_3)_2]\cdot 3H_2O$ (**2**), $\{(4,4'\text{-}H_2bpy)_2[(cis\text{-}Mo^{VI}O_2)_5(\mu_2\text{-}O)_5(\mu_5\text{-}SO_3)_2]\cdot H_2O\}_x$ (**3**), and $(NH_4)_7[(Mo_2{}^{V}O_2)Co^{III}(\mu_3\text{-}O)(\mu_2\text{-}O)(\mu_3\text{-}SO_3)(\mu_2\text{-}SO_3)_2(SO_3)_3(NH_3)]\cdot 4H_2O$ (**4**). Compound **3** exhibits chiral, NLO, and photoluminescence properties. The molybdenum(V)/cobalt(III)−sulfite species **4** is the first mixed-metal−sulfite cluster to date. A theoretical analysis of the geometry of the anion $[Mo_2{}^{V}Co^{III}S_6O_{22}(NH_3)]^{7-}$ of compound **4** on the basis of density functional theory (DFT) was also carried out, and the calculated vibrational frequencies have been used for the assignment of its vibrational spectrum.

Experimental Section

Materials. Reagent grade chemicals were obtained from Aldrich and used without further purification. C, H, N, and S analyses were conducted by the microanalytical service of the Department of Chemistry, University of Lisboa. Molybdenum and cobalt were determined by atomic absorption.

$(NH_4)_4[(cis\text{-}Mo^{VI}O_2)_4(\mu_4\text{-}O)(\mu_2\text{-}O)_4(\mu_4\text{-}\eta^2\text{:}\eta^2\text{-}O,O\text{-}SO_3)]\cdot H_2O$ (1). Solid $Na_2Mo^{VI}O_4\cdot 2H_2O$ (0.50 g, 2.07 mmol) was dissolved in aqueous HCl (37% HCl in water 1:4 v/v, 10 mL, pH = 0), and then acetonitrile (10 mL) was added to it. Subsequently solid $(NH_4)_2SO_3\cdot H_2O$ (5.00 g, 37.27 mmol) was slowly added in small portions under magnetic stirring. When the whole quantity of $(NH_4)_2SO_3\cdot H_2O$ was added to the solution, the colorless aqueous phase changed to yellow and its pH value was 5. The reaction mixture was left to crystallize at room temperature in an open vessel for 3 days. Colorless crystals of **1** were filtered out and dried in air. Yield: 0.20 g (51%, based on molybdenum). Anal. Calcd for $H_{18}N_4O_{17}SMo_4$: H, 2.38; N, 7.35; S, 4.21; Mo, 50.37. Found: H, 2.23; N, 7.51; S, 4.38; Mo, 50.85. FTIR (KBr, pellets, cm^{-1}): 3509 (m), 3434 (m), 3200 vb (m), 1641 (v), 1662 (vw), 1614 (w), 1425 sh (vs), 1409 (vs), 1043 (s), 932 (vs), 920 sh (vs), 855 (s), 808 (s), 693 br (s), 6001 (vw), 566 (w), 540 (w), 496 (w), 455 (vw).

$(NH_4)_4[(cis\text{-}Mo^{VI}O_2)_5(\mu_2\text{-}O)_5(\mu_5\text{-}\eta^2\text{:}\eta^2\text{:}\eta^1\text{-}O,O,O\text{-}SO_3)_2]\cdot 3H_2O$ (2). The same procedure as for the above compound **1** was followed to prepare **2** except that acetonitrile was not used. Yield: 70%, based on molybdenum. Anal. Calcd for $H_{22}N_4O_{24}S_2Mo_5$: H, 2.20; N, 5.57; S, 6.38; Mo, 47.69. Found: H, 2.15; N, 5.61; S, 6.28; Mo, 47.01. FTIR (KBr, pellets, cm^{-1}): 3143 (m), 1595 (w), 1402 (s), 1017 (m), 931 (s), 901 (vs), 868 (s), 828 (s), 680 (m), 619 (w), 534 (w), 492 (w), 415 (vw).

$(4,4'\text{-}H_2bipy)_2[(cis\text{-}Mo^{VI}O_2)_5(\mu_2\text{-}O)_5(\mu_5\text{-}\eta^2\text{:}\eta^2\text{:}\eta^1\text{-}O,O,O\text{-}SO_3)_2]\cdot H_2O$ (3). Solid $Na_2Mo^{VI}O_4\cdot 2H_2O$ (1.00 g, 4.13 mmol) was dissolved in aqueous HCl (37% HCl in water, 1:4 v/v, 50 mL, pH = 0), and then solid $(NH_4)_2SO_3\cdot H_2O$ (6.00 g, 44.72 mmol) was slowly added in small portions under magnetic stirring. When the whole quantity of $(NH_4)_2SO_3\cdot H_2O$ was added to it, the colorless solution changed to yellow and its pH value was 2.5. Subsequently an aqueous

(2) (a) Clemente-Juan, J.; Coronado, E. *Coord. Chem. Rev.* **1999**, *193−195*, 361 and references therein. (b) Botar, B.; Kögerler, P.; Hill, C. L. *Chem. Commun.* **2005**, 3138. (c) Botar, B.; Kögerler, P.; Müller, A.; Garcia-Serres, R.; Hill, C. L. *Chem. Commun.* **2005**, 5621. (d) Müller, A.; Todea, A-M.; Bögge, H.; Slageren, J.; Dressel, M.; Stammler, A.; Rusu, M. *Chem. Commun.* **2006**, 3066. (e) Botar, B.; Kögerler, P.; Hill, C. L. *J. Am. Chem. Soc.* **2006**, *128*, 5336.

(3) (a) Haushalter, R. C.; Mundi, L. A. *Chem. Mater.* **1992**, *4*, 31. (b) Peloux, C.; Dolbecq, A.; Mialane, P.; Marrot, J.; Riviere, E.; Secheresse, F. *Angew. Chem., Int. Ed.* **2001**, *40*, 2455. (c) Pouet, C. E.; Robert-Labarre, M. J. Peloux, C.; Marrot, C.; Secheresse, F. *J. Am. Chem. Soc.* **2004**, *126*, 9127.

(4) (a) Matsumoto, K. Y.; Kato, M.; Sasaki, Y. *Bull. Chem. Soc. Jpn.* **1976**, *49*, 106. (b) Manos, M. J.; Woollins, J. D.; Slawin, A. M. Z.; Kabanos, T. A. *Angew. Chem., Int. Ed.* **2002**, *41*, 2801. (c) Manos, M. J.; Miras, H. N.; Tangoulis, V.; Woollins, J. D.; Slawin, A. M. Z.; Kabanos, T. A. *Angew. Chem., Int. Ed.* **2003**, *42*, 425. (d) Long, D. L.; Kögerler, P.; Cronin, L. *Angew. Chem., Int. Ed.* **2004**, *43*, 1817. (e) Long, D. L.; Abbas, H.; Kögerler, P.; Cronin, L. *Angew. Chem., Int. Ed.* **2005**, *44*, 3415. (f) Miras, H. N.; Raptis, R. G.; Lalioti, N.; Sigalas, M.; Baran, P.; Kabanos, T. A. *Chem.−Eur. J.* **2005**, *11*, 2306. (g) Miras, H. N.; Raptis, R.; Baran, P.; Lalioti, N.; Harrison, A.; Kabanos, T. A. *C. R. Chim.* **2005**, *8*, 957. (i) Chilas, G. I.; Miras, H. N.; Manos, M. J.; Woollins, J. D.; Slawin, A. M.; Stylianou, M.; Keramidas, A. D.; Kabanos, T. A. *Pure Appl. Chem.* **2005**, *77*, 1529. (j) Baffert, C.; Boas, J. F.; Bond, A. M.; Kögerler, P.; Long, De-L.; Pilbrow, J. R.; Cronin, L. *Chem.−Eur. J.* **2006**, *12*, 8472. (k) Dolbecq, A.; Lisnard, L.; Mialane, P.; Marrot, J.; Bénard, M.; Rohmer, M.-M.; Sécheresse, F. *Inorg. Chem.* **2006**, *45*, 5898. (l) Fay, N.; Bond, A. M.; Baffert, C.; Boas, J. F.; Pilbrow, J. R.; Long, D.-L.; Cronin, L. *Inorg. Chem.* **2007**, *46*, 3502.

(5) (a) Sykora, R. E.; Ok, K. M.; Halasyamani, P. S.; Albrecht-Schmitt, T. E. *J. Am. Chem. Soc.* **2002**, *124*, 1951. (b) Chi, E. O.; Ok, K. M.; Porter, Y.; Halasyamani, P. S. *Chem. Mater.* **2006**, *18*, 2070.

(6) Astashkin, A. V.; Raitsimrig, A. M.; Feng, C. J.; Johnson, J. L.; Rajagopalan, K. V.; Enemark, J. H. *J. Am. Chem. Soc.* **2002**, *124*, 6109.

(7) (a) Estermann, M.; McCuster, L. B.; Baerlocher, C.; Merrouche, A.; Kessler, H. *Nature* **1991**, *352*, 320. (b) Huo, Q.; Xu, R.; Li, S.; Ma, Z.; Thomas, J. M.; Jones, R. H.; Chippindate, A.M. *J. Chem. Soc., Chem. Commun.* **1992**, 875.

(8) (a) Nguyen, Dan-Tam.; Chew, E.; Zhang, Q.; Choi, A.; Bu, X. *Inorg. Chem.* **2006**, *45*, 10722. (b) Nguyen, Dan-Tam.; Bu, X. *Inorg. Chem.* **2006**, *45*, 10410. (c) Rao, K. P.; Rao, C. N. R. *Inorg. Chem.* **2007**, *46*, 2511.

(9) Gibney, S. C.; Ferraudi, G.; Shang, M. *Inorg. Chem.* **1999**, *38*, 2898.

(10) (a) Armatas, N. G.; Burkholder, E.; Zubieta, J. *J. Solid State Chem.* **2005**, *178*, 2430. (b) Lisnard, L.; Dolbecq, A.; Mialane, P.; Marrot, J.; Codjovi, E.; Sécheresse, F. *Dalton Trans.* **2005**, 3913. (c) Ritchie, C.; Burkholder, E.; Kögerler, P.; Cronin, L. *Dalton Trans.* **2006**, 1712. (d) Streb, C.; Long D.-L.; Cronin, L. *Chem. Commun.* **2007**, 471.

Table 1. Crystallographic Data for Compounds **1**, **3**, and **4**

param	**1**	**3**	**4**
empirical formula	$H_{18}N_4O_{17}SMo_4$	$C_{10}H_{11}N_2O_{11}S_1Mo_{2.5}$	$H_{39}N_8O_{26}S_6Mo_2Co$
fw (calcd)	761.99	607.12	1010.56
temp (K)	293 (2)	100 (2)	100 (2)
wavelength (Å)	0.710 73	0.710 73	0.710 73
cryst system	triclinic	monoclinic	triclinic
space group	$P\bar{1}$	$C2$	$P\bar{1}$
a (Å)	6.9748 (7)	20.2774 (16)	9.2703 (7)
b (Å)	7.6523 (8)	10.68.56 (7)	12.3786 (8)
c (Å)	16.8584 (16)	8.6685 (7)	14.3790 (9)
α (deg)	95.184 (8)	90	76.130 (5)
β (deg)	94.376 (8)	113.960 (8)	72.426 (6)
γ (deg)	95.542 (8)	90	81.135 (6)
V (Å^3)	888.63 (15)	1716.4 (2)	1521.20(18)
Z	2	4	2
density (calcd, mg/m^3)	2.780	2.349	2.206
abs coeff (mm^{-1})	2.963	1.993	1.871
R1 [$I > 2\sigma(I)$]	0.0429	0.0177	0.0157
wR2 [$I > 2\sigma(I)$]	0.1213	0.0364	0.0427

solution (100 mL) containing 4,4′-bipyridine[11a] (0.28 g, 1.79 mmol) was added dropwise[11b] to the above solution under magnetic stirring. Colorless crystals of **3** started to form 10 min later, and their formation was completed within 1 h. The crystals were filtered out and dried in air. Yield: 0.85 g (85%, based on molybdenum). Anal. Calcd for $C_{20}H_{22}N_4O_{22}S_2Mo_5$: C, 19.79; H, 1.82; N, 4.61; S, 5.28; Mo, 39.51. Found: C, 19.80; H, 1.75; N, 4.85; S, 5.12; Mo, 39.15. FTIR (KBr, pellets, cm^{-1}): 3492 (m), 3443 (m), 3231 (vw), 3088 (m), 3068 (m), 2591 vb (w), 2363 (vw), 2350 (vw), 2091 (w), 2115 (vw), 1631 sh (m), 1616 (m), 1495 (m), 1382 (w), 1242 (vw), 1209 (w), 1104 sh (vw), 1027 (s), 1003 (w), 906 (vs), 887 (vs), 872 (s), 826 (s), 798 (s), 690 sh (s), 678 (s), 532 (m), 532 (w), 492 (m), 421 (vw).

$(NH_4)_7[(Mo^V_2O_2)Co^{III}(\mu_3$-O)$(\mu_2$-O)$(\mu_3$-$\eta^1$:$\eta^1$:$\eta^1$-*O,O,S*-$SO_3)(\mu_2$-$\eta^1$:$\eta^1$-*O,S*-$SO_3)_2(\eta^1$-*O*-$SO_3)_2(\eta^1$-*S*-$SO_3)(NH_3)]\cdot 4H_2O$ (4). To a stirred solution of aqueous HCl (37% HCl in water, 1:4 v/v, 25 mL) containing $Na_2Mo^{VI}O_4\cdot 2H_2O$ (0.50 g, 2.07 mmol) and $Co^{II}Cl_2\cdot 6H_2O$ (0.50 g, 2.10 mmol) was added solid $(NH_4)_2SO_3\cdot H_2O$ (8.10 g, 60.38 mmol) slowly in small portions. Upon addition of $(NH_4)_2SO_3$, a sequence of color changes (from light pink through orange-pink, orange, brown-orange to wine red) was induced and the pH of the solution changed from 0 to 5.3. At pH $\approx$ 4.8, an orange-red precipitate[11c] was formed which was redissolved upon further addition of $(NH_4)_2SO_3\cdot H_2O$. The reaction mixture was left to crystallize at room temperature in open test tubes (diameter 1 cm) for 3 days to give orange-red[11d] and red crystals,[11d] which were filtered out and dried in air. The orange-red crystals of compound **4** were manually separated readily under a microscope. Yield: 0.20 g (20%, based on molybdenum). Anal. Calcd for $H_{39}N_8O_{26}S_6CoMo_2$: H, 3.89; N, 11.09; S, 19.04; Co, 5.78; Mo, 18.15. Found: H, 3.71; N, 11.14; S, 19.25; Co, 5.83; Mo, 18.70. The quantity of red crystals (compound **5**), which were of very poor quality, was 0.41 g and gave the following elemental analysis: H, 4.40; N, 11.30; S, 22.11; Co, 16.49; Na, 0.83. On the basis of the elemental analysis compound **5** should have the following empirical formula: $H_{12}N_{22}S_{19}Co_8Na$. The infrared spectra of compounds **4** and **5** are shown in Figure S1 (Supporting Information).

X-ray Crystallography. A Siemens SMART Platform CCD diffractometer operating at room temperature and using graphite-monochromatized Mo Kα radiation was used for data collection of compound **1**. Cell refinement and data reduction were carried out with the program SAINT.[12] An empirical absorption correction was done to the data using SADABS.[12] The intensities were extracted by the program XPREP.[13] The structures were solved with direct methods using SHELXS, and least-square refinement was done against F^2 using routines from SHELXTL software.[13] The hydrogen atoms were located in a difference Fourier map and refined only isotropically. The intensity data for compounds **3** and **4** were collected on an Oxford XCalibur 4-cycle diffractometer using Mo Kα ($\lambda = 0.7107$ Å) radiation. Each structure was solved by direct methods using program SHELX-97[14] and refined by full-matrix least-squares techniques.[15] All the non-hydrogen atoms of **3** and **4** were refined anisotropically, while the hydrogen atoms, all found in the ΔF map, were refined with isotropic thermal parameters. Crystallographic data for compounds **1**, **3**, and **4** are given in Table 1.

Physical Measurements. IR spectra of the various compounds dispersed in KBr pellets and in Nujol with CsI windows were recorded on a Perkin-Elmer Spectrum GX FT-IR spectrometer. Magnetic moments were measured at room temperature by the Faraday method, with mercuric tetrathiocyanatocobaltate(II) as the susceptibility standard on a Cahn-Vetron RM-2 balance. Continuous-wave EPR spectra were recorded at liquid-helium temperatures (20 K) with a Bruker ER 200 D X-band (9.42 GHz) spectrometer equipped with an Oxford Instruments cryostat. The solid-state circular dichroism (CD) spectrum of compound **3** was run on a Jasco 720 spectropolarimeter.

Computational Details. Density functional theory calculations were performed with the Gaussian 03 set of programs,[16] using the B3PW91 functional.[17,18] The transition metal atoms were represented by the relativistic effective core potential (RECP) from the

(11) (a) The solid 4,4′-bipy was added very slowly in small portions to the stirred aqueous solution in order to be dissolved. (b) The aqueous solution containing the 4,4′-bipy was added dropwise to Mo^{VI}/SO_3^{2-} system to get very good quality crystals of **3**. In contrast, quick addition of it results in the formation of very poor quality crystals of **3** or a precipitate of **3**. (c) Sometimes the orange-red precipitate is not formed. (d) Occasionally crystals of **4** or **5** are formed exclusively and not a mixture of **4** and **5**. Thus far, we have not been successful in determining the factors which lead to the formation of **4** or **5** or to the mixture of **4** or **5**. (e) A possible role of the CH_3CN in the formation of compound **1** might be the reduction of polarity of the solvent system.

(12) Siemens Analytical X-Ray Instruments Inc., 1995.
(13) Sheldrick, G. M. *SHELXTL, Crystallographic Software Package, SHELXTL*, version 5.1; Bruker-AXS: Madison, WI, 1998.
(14) Sheldrick, G. M. *SHELXL-97: Program for the Refinement of Crystal Structure*; University of Gottingen: Gottingen, Germany, 1997.
(15) Sheldrick, G. M. *SHELXS-86: Program for the Solution of Crystal Structure*; University of Gottingen: Gottingen, Germany, 1990.
(16) Pople, J. A.; et al. *Gaussian 03*, revision B.02; Gaussian, Inc.: Pittsburgh, PA, 2003.
(17) Becke, A. D. *J. Chem. Phys.* **1993**, *98*, 5648.
(18) Perdew, J. P.; Wang, Y. *Phys. Rev. B* **1992**, *45*, 13244.

Scheme 1. Synthetic Routes to Isolated Compounds **1**−**5**

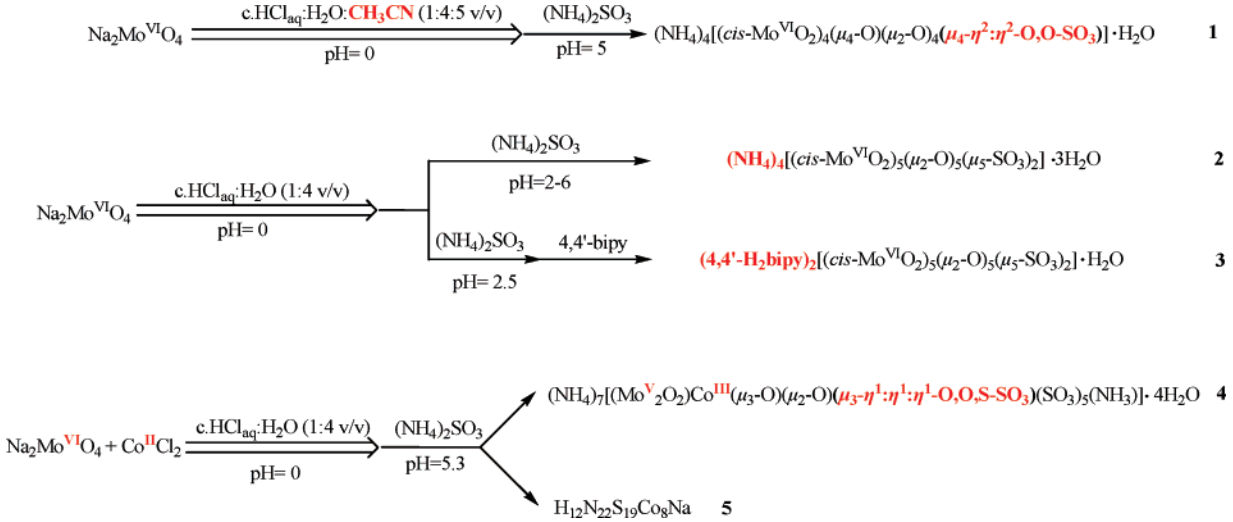

Stuttgart group and their associated basis set,[19,20] augmented by an f polarization function ($\alpha = 2.2$, Co; $\alpha = 1.043$, Mo).[21] The sulfur atom was represented by RECP from the Stuttgart group and the associated basis set,[22] augmented by a d polarization function ($\alpha = 0.503$).[23] A 6-31G(d,p) basis set was used for all the remaining atoms of the molecules studied (H, O, N).[24] The geometry optimizations were performed without any symmetry constraint followed by analytical frequency calculations to confirm that a minimum had been reached.

Thermal Analyses. Thermogravimetric analyses (TGA) of the samples were performed using a NETZSCH apparatus (model STA449C Jupiter) from ambient temperature (∼20 °C) to 600 °C, with heating rate of 5 °C/min, in a nitrogen atmosphere (45 mL/min).

Nonlinear Optical Measurements. The powder second harmonic generation (SHG) measurements have been performed using a modified Kurtz-Perry NLO system.[25] The thin (∼200 μm) powder layers of the materials studied were irradiated by a Nd:YAG laser (Quantel YG-901C) that produces 35 ps pulses at 1064 nm, at a repetition rate of 10 Hz. The generated green light was analyzed by a monochromator equipped with a CCD camera (SBIG-ST6B) connected to a PC where the data were stored. Thus, the production of the second harmonic was verified by the observation of a single peak at 532 nm in the recorded spectra and its quadratic dependence on laser intensity. Moreover, the intensity of this peak was used to make relevant comparison of the SHG efficiency of compound **3** with respect to urea. The relative efficiency ratio has been determined for various numbers of pulses and laser intensities below the damage thresholds. The laser intensity damage threshold was determined as the lower laser intensity, which causes decomposition (sample darkening) of the studied material after few laser pulses and effects the SHG efficiency.

Solid-State UV−Vis/NIR Reflectance and Photoluminescence Spectroscopy. UV−vis/near-IR diffuse reflectance spectra were obtained at room temperature on a Shimadzu UV-3101PC double-beam, double-monochromator spectrophotometer in the wavelength range 200−2500 nm. $BaSO_4$ powder was used as a reference (100% reflectance) and base material on which the powder sample was coated. Reflectance data were converted to absorbance data as described elsewhere.[26] Photoluminescence (PL) spectra were obtained on a Spex Fluorolog-2 F111AI spectrofluorometer. Samples were loaded into 3 mm silica tubes, and excitation and emission spectra were recorded at 77 K.

Results and Discussion

Syntheses. The synthesis of the molybdenum−sulfite compounds **1**−**5** is summarized in Scheme 1. Addition of acetonitrile to the molybdenum(VI)−sulfite system resulted in the isolation of compound **1**, $(NH_4)_4[Mo_4^{VI}SO_{16}]\cdot H_2O$, in which the ratio of molybdenum to sulfite (Mo:S) is 4 to 1, while in water:*c*HCl(aq) (4:1 v/v) compound **2**, $(NH_4)_4[Mo_5^{VI}S_2O_{21}]\cdot H_2O$, was isolated instead with a Mo:S ratio of 5 to 2; in other words, compound **2** is richer in sulfur than compound **1**. Thus, it is reasonable to assume that the role of the acetonitrile is the reduction of the sulfite concentration into the solution. To investigate this assumption a series of experiments was conducted by changing the molar ratio of molybdenum/sulfite. Consequently, the syntheses in acetonitrile/water:*c*HCl(aq) (1:4 v/v) and in acidic aqueous solution were conducted at pH values 4, 5, and 6 by simply changing the quantity of $(NH_4)_2SO_3$, since the higher the concentration of SO_3^{2-} the higher the pH value of the solution and vice versa. In all the pH values compounds **1** and **2**[27] were isolated respectively as it was evidenced by IR spectroscopy. Therefore, it is crystal clear that the molybdenum/sulfite molar ratio does not play a crucial role in the isolation of **1** and **2**, and so, the role of acetonitrile in the isolation of **1** is unidentified.[11e] Compound **2** was prepared by Sasaki and co-workers[4a] by another procedure, namely as follows: An aqueous solution of $(NH_4)_6[Mo_7^{VI}O_{24}]$ was

(19) Dolg, M.; Wedig, U.; Stoll, H.; Preuss, H. *J. Chem. Phys.* **1987**, *86*, 866.
(20) Andrae, D.; Haüssermann, U.; Dolg, M.; Stoll, H.; Preuss, H. *Theor. Chim. Acta* **1990**, *77*, 123.
(21) Ehlers, A. W.; Böhme, M.; Dapprich, S.; Gobbi, A.; Höllwarth, A.; Jonas, V.; Köhler, K. F.; Stegmann, R.; Veldkamp, A.; Frenking, G. *Chem. Phys. Lett.* **1993**, *208*, 111.
(22) Bergner, A.; Dolg, M.; Küchle, W.; Stoll, H.; Preuss, H. *Mol. Phys.* **1993**, *80*, 1431.
(23) Höllwarth, A.; Böhme, H.; Dapprich, S.; Ehlers, A. W.; Gobbi, A.; Jonas, V.; Köhler, K. F.; Stegmann, R.; Veldkamp, A.; Frenking, G. *Chem. Phys. Lett.* **1993**, *203*, 237.
(24) Hariharan, P. C.; Pople, J. A. *Theor. Chim. Acta* **1973**, *28*, 213.
(25) Kurtz, S. K.; Perry, T. T. *J. Appl. Phys.* **1968**, *39*, 3798.
(26) McCarthy, T. J.; Ngeyi, S. P.; Liao, J. H.; Degroot, D. C.; Hogan, T.; Kannewurf, C. R.; Kanatzidis, M. G. *Chem. Mater.* **1993**, *5*, 331.
(27) Compound **2** was also isolated at pH value of 2.5.

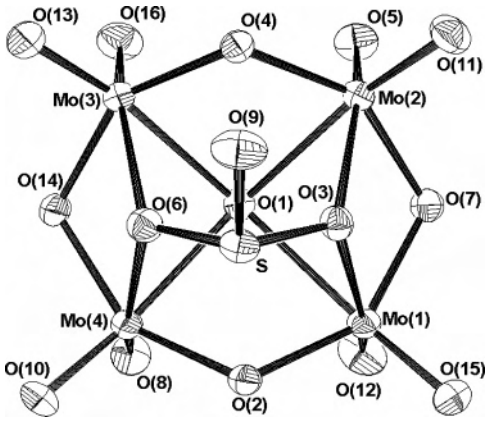

Figure 1. ORTEP representation of the anion of **1**.

saturated with sulfur dioxide and immediately cooled to get **2**. When the same solution was kept in a desiccator at room temperature, the authors claim the isolation of compound $(NH_4)_6[Mo_8^{VI}S_2O_{31}]\cdot 5H_2O$ (**2′**), without reporting any physicochemical data. Our efforts to prepare **2′** by changing the molar ratio of Mo^{VI}/SO_3^{2-}, pH (vide supra), temperature, and metal source $\{Na_2Mo^{VI}O_4$ and $(NH_4)_6[Mo_7^{VI}O_{24}]\}$ were unsuccessful, and compound **2** was isolated in all cases. Dropwise addition[11b] of 4,4′-bipyridine dissolved in water[11a] to an acidic (pH = 2.5) aqueous solution of Mo^{VI}/SO_3^{2-} resulted in the isolation of crystals of compound **3** suitable for X-ray structure analysis. Although the hybrid framework compound **3** has the same molybdenum sulfite building block, $[Mo_5S_2O_{21}]^{4-}$, with **2** its physical properties have changed dramatically [thermal stability, SHG, and photoluminescence properties (vide infra)]. When cobalt(II) was introduced to the molybdenum(VI)/sulfite system, a completely new chemistry emerged with the isolation of the novel trinuclear $[Co^{III}Mo_2^{V}-$sulfite] species (**4**), along with a cobalt/sulfite species (**5**). Unfortunately, the crystals of compound **5** were twins and of very poor quality to allow the solution of the X-ray crystal structure of **5**. Our efforts to get better quality crystals of **5** and to prepare compounds **4** and **5** as pure phases by changing the molar ratio of Mo^{VI}/Co^{II}, pH, temperature (in the range 20−60 °C), and metal source of molybdenum $\{Na_2Mo^{VI}O_4$, $(NH_4)_6[Mo_7^{VI}O_{24}]$, and $Mo^{VI}O_3\}$ were unsuccessful thus far. Efforts to resolve the matter are underway. At this point, two features are worth noting: (1) The sulfite anion does not reduce molybdenum(VI) to molybdenym(V) irrespective of conditions used (pH, solvent system, and counterions). (2) In marked contrast, the presence of cobalt(II) in the molybdenum(VI)/sulfite system causes the reduction of Mo^{VI} to Mo^{V}. The driving force for this redox reaction might be the thermodynamic stability of cobalt(III) atom ligated to sulfur atoms.

Crystal Structures. X-ray structural analysis of **1** revealed the presence of the discrete cluster $[(cis\text{-}Mo^{VI}O_2)_4(\mu_4\text{-}O)(\mu_2\text{-}O)_4(\mu_4\text{-}SO_3)]^{4-}$ (Figure 1) as well as four ammonium counterions and a water molecule of crystallization. A selection of interatomic distances relevant to the molybdenum coordination spheres in **1** is listed in Table S1 (Supporting Information). The anion consists of four alternately face- and edge-sharing octahedra capped by the sulfite group which bridges the apexes of the face-sharing octahedra. Three kinds of oxygen atoms exist in the cluster according to the way the oxygen atoms are coordinated: terminal oxygen O_t; double-bridging oxygen $O(\mu_2)$; four-bridging oxygen $O(\mu_4)$. Thus, the average Mo−O bond lengths fall into three classes: Mo−O_t = 1.703 ± 0.004 Å; Mo−$O(\mu_2)$ = 1.911 ± 0.022 Å; Mo−$O(\mu_4)$ = 2.393 ± 0.092 Å. The sulfur(IV) atom of the sulfite group adopts its characteristic pyramidal coordination, with the stereochemically active pair of electrons presumably directed toward the fourth tetrahedral vertex, like $Se^{IV}O_3^{2-}$ reported in the literature.[28] The average S−O bond length of 1.569(4) Å for S−O(3) and S−O(6) is in good agreement with previous studies.[4] The terminal S−O(9) bond is short [1.493(4) Å], indicating that the oxygen atom is not protonated [BVS (bond valence sum) for O(9) = 1.8]. BVS[29,30] calculations indicate that the molybdenum atoms are in the +6 oxidation state, confirmed by the particular coordination environment of Mo(VI) atoms, while the sulfur and the μ_4-oxygen atoms are in the oxidation states +4 and +2, respectively. The four molybdenum atoms form a rectangle of average dimensions of 3.3173(8) × 3.1958(6) Å and average Mo−Mo−Mo angles of 88.589(15), 90.926(16), 88.941(15), and 91.539(16)°. The shorter edges are between face-sharing molybdenum octahedra. At the base of the anion is an oxygen O(1) that is simultaneously shared by all four molybdenum atoms. Three of the four Mo−O distances average 2.293 Å, but the fourth is considerably longer [2.485(4) Å], in marked contrast to its selenium analogue,[31] $[Mo_4^{VI}O_{13}(Se^{IV}O_3)]^{4-}$, where the four Mo−$\mu_4$-O distances are almost identical [average d(Mo−O) = 2.401 Å]. The results of a least-square plane calculation involving the four molybdenum atoms indicate that no molybdenum atom is more than 0.0077(4) Å from a plane. Each molybdenum atom deviates 0.0077(4) Å from the mean plane defined from the four molybdenum atoms, while O(1) is 0.747(4) Å below the plane of the four molybdenum atoms. The tetranuclear cluster, $[Mo^{VI}O_{12}(\mu_4\text{-}O)(SO_3)]^{4-}$, i.e. the anion of compound **1**, resembles with the tetranuclear organoclusters of the general formula $[Mo_4^{VI}O_{12}(\mu_4\text{-}OH)(\mu_4\text{-}O_2X)]^{3-}$ (X = $-CH_2-$, R_2As-, etc).[32] In the latter tetranuclear clusters the μ_4-oxygen of the hydroxyl group forms three almost equidistant Mo−O bonds (∼2.40 Å) and a longer one (∼2.54 Å), a situation very similar with the anion of **1**.

The crystal structure of **3** is constructed from $[(cis\text{-}Mo^{VI}O_2)_5(\mu_2\text{-}O)_5(\mu_5\text{-}SO_3)_2]^{4-}$ clusters (Figure 2). A selection of interatomic distances relevant to the molybdenum coordination spheres in **1** is listed in Table S2. Neighboring

(28) Kortz, U.; Savelieff, M. G.; Abou Ghali, F. Y.; Khalil, L. M.; Maalouf, S. A.; Sinno, D. *Angew. Chem., Int. Ed.* **2002**, *41*, 4070−4073.
(29) Brown, I. D.; Altermatt, D. *Acta Crystallogr., Sect. B* **1985**, *41*, 244.
(30) Brese, N. E.; O'Keeffe, M. *Acta Crystallogr., Sect. B* **1991**, *47*, 192.
(31) Feng, M. L.; Mao, J. G. *Eur. J. Inorg. Chem.* **2004**, 3712−3717.
(32) (a) Barkigia, K. M.; Rajkovic, L. M.; Pope, M. T.; Quicksall, C. Q. *J. Am. Chem. Soc.* **1975**, *97*, 4146−4147. (b) Matsumoto, K. Y. *Bull. Chem. Soc. Jpn.* **1979**, *52*, 3284−3291. (c) Day, V. W.; Fredrich, M. F.; Liu, L. S.; Klemperer, W. G. *J. Am. Chem. Soc.* **1979**, *101*, 491−492. (d) Day, V. W.; Thompson, M. R.; Klemperer, W. G.; Liu, R. S. *J. Am. Chem Soc.* **1980**, *102*, 5971−5973. (e) Barkigia, K. M.; Rajkovic, L. M.; Pope, M. T.; Prince, E.; Quicksall, C. Q. *Inorg. Chem.* **1980**, *19*, 2531−2537.

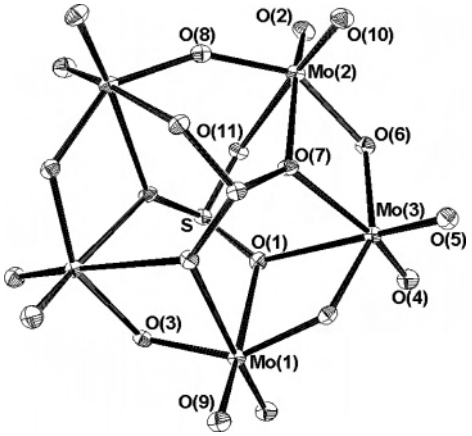

Figure 2. ORTEP representation of the anion of **3**.

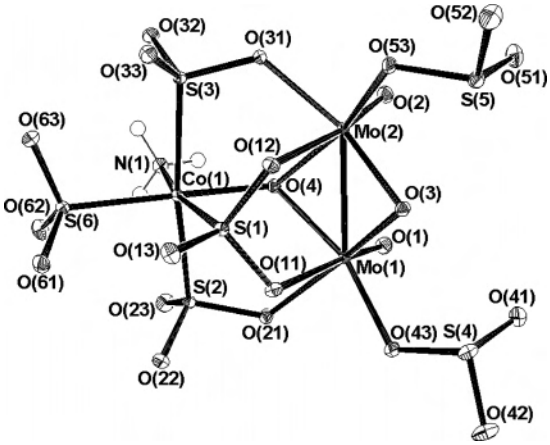

Figure 3. ORTEP representation of the anion of **4**.

$[Mo^{VI}_5S_2O_{21}]^{4-}$ clusters are linked together with strong hydrogen bonds (Table S3) between the two hydrogen atoms of the water molecule, $H_2O(12)$, and the sulfite oxygen atoms O(11) of each cluster to form infinite chains running along [001] (Figure S2A). The chains are linked through diprotonated 4,4′-bipyridine cations (4,4′-H_2bipy^{2+}) into a three-dimensional architecture (Figure S2A). Each molybdosulfite building block, $[Mo^{VI}_5S_2O_{21}]^{4-}$, employs two terminal oxo groups [O(9) and O(9)′] of Mo(1) and two bridging (μ_2-) oxo groups [O(6) and O(6)′] (Figure 2SB) to form four strong hydrogen bonds (Table S3) with the protons attached to the nitrogen atoms which belong to four distinct diprotonated bipyridines. The H_2bipys^{2+} are lying around the water hydrogen-bonded $[Mo^{VI}_5S_2O_{21}]^{4-}$ chains in a helicoidal manner giving rise to the chiral properties of the bulk material. The H_2bipy^{2+} exhibits a 36.3(2)° right-handed twist angle between the rings (*R*-conformation) of the bipyridyl units. The $[Mo_5S_2O_{21}]^{4-}$ anion consists of five distorted {MoO_6}octahedra which form a ring. The octahedra are joined through common edges, except one contact between the octahedra of Mo(2) and its symmetry-related Mo(2)′ that share a corner. Two SO_3^{2-} trigonal pyramids are attached to the ring, one above and the other below it. BVS calculations revealed that all the molybdenum atoms are in the +6 oxidation state, confirmed by the particular coordination environment of Mo(VI) atoms, and the sulfur atoms in the +4 oxidation state. The Mo^{VI}_5 cluster belongs to C_2 symmetry group with the Mo(1) and O(8) atoms to define the C_2 axis. The C_2 symmetry group is dissymmetric, and thus the cluster exhibits two enantiomers. However, only one of the two possible enantiomers is present in the structure of **3**. If one looks along the axis defined by the two S atoms, the S−O(1)−Mo(1)−O(1)−S, S−O(11)−Mo(2)−O(7)−S, and S−O(11)−Mo(2)−O(7)−S rings form a right-handed helix, and using the nomenclature applied to inorganic complexes, the enantiomer could be named as Δ-. The chiral properties of *R*-4,4′-bipy and of the $[Mo_5S_2O_{21}]^{4-}$ cluster give rise to the unit cell asymmetry of the structure and are responsible for the NLO properties of compound **3**. The structure of the Strandberg-type cluster $\{Mo^{VI}_5S_2O_{21}\}^{4-}$ is almost identical with that reported by Matsumoto[4a] and co-workers in compound $(NH_4)_4[Mo^{VI}_5S_2O_{21}]\cdot 3H_2O$ (**2**) and very similar to those reported in Mo^{VI}_5 clusters with PO_4^{3-}, SO_4^{2-}, etc.[33]

As shown in Figure 3, the anion of **4** is a trinuclear mixed-metal $[Co^{III}Mo_2^{V}]$ species. A selection of interatomic distances and angles relevant to the cobalt and molybdenum coordination spheres in **4** is listed in Table S4. The octahedral cobalt(III) unit is coordinated to $[Mo^{V}_2O_4]^{2+}$ core through one μ_3-O^{2-}, two μ_2-SO_3^{2-} (*S*,*O*), and one μ_3-SO_3^{2-} (*S*,*O*,*O*) bridges. Each molybdenum(V) atom is ligated in a severely distorted {MoO_6} octahedral coordination geometry (ignoring the $Mo^{V}-Mo^{V}$ bond) to one μ_2- and one μ_3-O^{2-} ions, three sulfite (one terminal, one μ_2-*S*,*O*, and one μ_3-*S*,*O*,*O*) oxygen atoms, and an oxo group. The cobalt(III) atom possesses a severely distorted {$CoNOS_4$} octahedral coordination and is ligated to four sulfite [one terminal, two μ_2-SO_3^{2-} (*S*,*O*), and a μ_3-SO_3^{2-} (*S*,*O*,*O*)] sulfur atoms, as well as one μ_3-O^{2-} ion and an ammonia nitrogen atom. The hydrogen atoms of the ligated to cobalt(III) ammonia molecule form intramolecular hydrogen bonds with the sulfite oxygens (Table S3). There is also an extensive intermolecular, hydrogen-bonding network between the ammonium and water hydrogen atoms and the sulfite and water oxygens and oxo groups. At this point, it is worth noting that compound **4** can be viewed as formed from the interaction of the cluster $\{[cis\text{-}Mo^{V}_2O_2(\mu_2\text{-}O)_2](\mu_2\text{-}\eta^1\text{:}\eta^1\text{-}O,O\text{-}SO_3)(SO_3)_4\}^{8-}$ (**6**) with cobalt(III). The isolation and structural characterization of cluster **6** with ammonium as counterions was reported in the literature.[4b] BVS calculations revealed that the oxidation state of molybdenum atoms is +5, confirmed by the particular coordination environment of Mo^{V} atoms, and of cobalt and sulfur atoms +3 and +4, respectively. In the $[Mo_2^{V}O_2(\mu_2\text{-}O)_2]^{2+}$ unit the molybdenum atoms have d^1 electronic configuration, but this unit does not contribute to the magnetic moment of **4** due to the strong metal−metal bond

(33) (a) Strandberg, R. *Acta Chem. Scand.* **1973**, *27*, 1004−1018. (b) Hori, T.; Himeno, S.; Tamada, O. *J. Chem. Soc. Dalton Trans.* **1992**, 275−280. (c) Burholder, E.; Golub, V.; O' Connor, C. J.; Zubieta, J. *Chem. Commun.* **2003**, 2128. (d) Fu, R. B.; Wu, X. T.; Hu, S. M.; Zhang, J. J.; Fu, Z. Y.; Du, W. X.; Xia, S. Q. *Eur. J. Inorg. Chem.* **2003**, 1798. (e) Kortz, U.; Marquer, C.; Thouvenot, R.; Nierlich, M. *Inorg. Chem.* **2003**, *42*, 1158. (f) Burholder, E.; Golub, V.; O' Connor, C. J.; Zubieta, J. *Inorg. Commun.* **2003**, *42*, 6729. (g) Shinvaiah, V.; Arumuganathan, T.; Das, S. K. *Inorg. Chem. Commun.* **2004**, *7*, 365.

Scheme 2 New Bonding Modes a and b of the Sulfite Anion

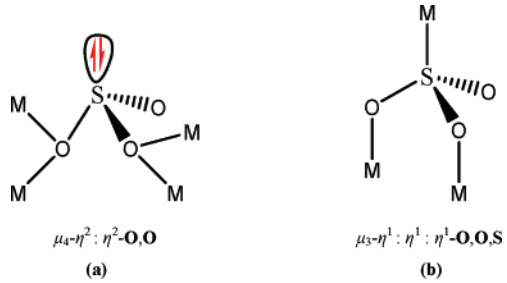

μ_4-η^2 : η^2-O,O (a) μ_3-η^1 : η^1 : η^1-O,O,S (b)

[d[(Mo(1)−Mo(2)] = 2.5855(3) Å in **4**]. Cobalt in oxidation +3 has a d^6 electronic configuration. The theory predicts (vide infra) that the low-spin octahedral Co^{III} configuration is very stable, and thus, compound **4** should be diamagnetic. This observation was confirmed by the magnetic susceptibility and cw EPR measurements of **4**, which gave a μ_{eff} value of 0 and no cw EPR signal. Therefore, it is crystal clear that the oxidation state of cobalt in **4** is unambignously +3, because if it was +2, compound **4** should be paramagnetic with a magnetic moment and an EPR signal, irrespective of low or high spin of a d^7 system.

New Bonding Modes of the Sulfite Anion. To the best of our knowledge, the bonding modes a and b, shown in Scheme 2, of the sulfite anion in the compounds **1** and **4**, respectively, are the first examples of such coordination modes for the sulfite anion. At this point, it is worth noting that when we embarked on the synthesis of metal/sulfite compounds almost 6 years ago, there was only a very limited number of coordination modes of the sulfite anion to the metal atoms, namely 7.[4b] Today, this number has been almost doubled.[4] Looking at the bonding modes[34] of the carbonate (CO_3^{2-}) anion, which has also three oxygens as donor atoms, though carbonate is a planar species, and taking into account that the sulfite anion has four potential donor atoms (S, O, O, O), one might expect a substantial increase of the bonding modes of the sulfite anion in the near future and, consequently, a substantial increase in the metal/sulfite compounds.

Thermal Analysis. The thermal properties of the four compounds (**1**−**4**) were investigated by TGA under nitrogen atmosphere and summarized in Table 2 (Figure S3). The thermal decomposition of compound **1** occurs in three main stages (Table 2). The first step takes place at 100−190 °C and is attributed to the removal of the crystalline water molecule and two ammonia molecules. The removal of the other two ammonia molecules and of the sulfur dioxide molecule occurs at a second stage (190−260 °C), while the dehydroxylation of **1** takes place at a third stage (260−420 °C) resulting in the formation of $Mo^{VI}O_3$. The experimental (calculated) percentage weight loss for the three stages are 6.80 (6.83), 12.83 (12.88), and 4.83 (4.73), respectively. Compound **2** has a thermal behavior very similar to that of compound **1** (Table 2). This is reasonable since both molybdenum compounds have oxo and sulfite ligands and ammonium as counterions. In contrast, compound **3** shows only two steps of weight loss at 200−370 and 370−520 °C. The first step corresponds to the loss of the crystalline water molecule and of one 4,4-bipy, while the second one to the loss of the second 4,4-bipy and of the two sulfur dioxide molecules and to the dehydroxylation of **3** per formula resulting in the formation of the corresponding metal oxide $Mo^{VI}O_3$. The experimental (calculated) percentage weight losses for the two stages are 14.00 (14.03) and 26.30 (25.80), respectively. The substitution of the ammonium in **2** for 4,4′-H_2bipy^{2+} counterions in **3** increases its thermal stability up to 200 °C and changes its thermal behavior in comparison to **1** and **2**. The TGA data for **4** reveal two weight losses at 70−120 and 120−460 °C corresponding to the removal of three crystalline water molecules and of the last crystalline water, eight ammonia, and six sulfur dioxide molecules as well as 3.5 H_2O (dehydroxylation), respectively, per formula unit resulting in the formation of the metal oxides 0.5 $Co^{III}_2O_3$ $Mo^{V}_2O_5$. The experimental (calculated) percentage weight losses for the two stages are 5.23 (5.35) and 59.29 (59.53), respectively.

Table 2. Thermal Properties of Compounds **1**−**4**

compd	wt loss[a] (%)	temp range (°C)	assgnt
1	6.80 (6.83)	100−190	H_2O + 2 NH_3
	12.83 (12.88)	190−260	2 NH_3 + SO_2
	4.83 (4.73)	260−420	2 H_2O[b]
2	5.00 (5.37)	100−180	3 H_2O
	13.15 (13.14)	180−280	4 NH_3 + SO_2
	9.15 (9.85)	270−580	SO_2 + 2 H_2O[b]
3	14.00 (14.03)	200−370	H_2O + 4,4′-bipy
	26.30 (25.80)	370−520	4,4′-bipy + 2 SO_2 + 2 H_2O[b]
4	5.23 (5.35)	70−120	3 H_2O
	59.29 (59.53)	120−460	H_2O + 8 NH_3 + 6 SO_2 + 3.5 H_2O[b]

[a] Values in parentheses are the calculated percentage for the weight loss of the molecules reported on the right column. [b] Water molecules from the dehydroxylation of compounds.

Nonlinear Optical Properties. The noncentrosymmetric structure of **3** implies that compound **3** is expected to have nonlinear optical properties. This is verified by the powder SHG measurements. The SHG efficiency found to be ∼4% of that of urea. It comes out that this corresponds to a SHG efficiency of approximately 15 times that of quartz. The intensity damage threshold was found to be ∼350 MW/cm^2, which is one order of magnitude higher than the values reported for other thio-containing compounds.[35] The solid-state CD spectrum of **3** at 180−350 nm did not give any peaks.

UV−Visible Spectra and Photoluminescence. Solid UV−visible spectra of phase-pure samples of **1**−**3** showed a broad band centered at 230, 280, and 260 nm for **1**−**3**, respectively, while compound **4** showed four peaks at 2430, 2130, 1560, and 350 nm and three shoulders at 2050, 1800, and 500 nm. The colorless compound **3** shows an optical energy gap of 3.34 eV (Figure 4), which indicates that it is a wide-band gap semiconductor. Compound **3** emits blue light when excited with energy close to its band gap. More specifically, compound **3** displays photoluminescence at 465 nm (2.6 eV) when excited at 374 nm (3.32 eV)

(34) Cotton, F. A.; Wilkinson, G.; Murillo, C. A.; Bochmann, M. *Advanced Inorganic Chemistry*, 6th ed.; John Wiley and Sons, Inc.: New York, 1999; p 484.

(35) Kim, Y.; Martin, S.; Min Ok, K.; Halasyamani, P. S. *Chem. Mater.* **2005**, *17*, 2046.

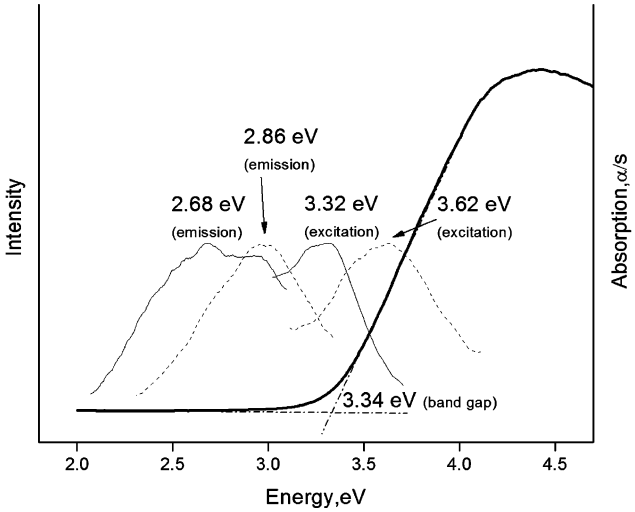

Figure 4. Optical energy gap of compound **3**. Black solid line: Optical absorption spectrum of compound **3**. Grey solid lines: Solid-state excitation and emission spectra of **3** recorded at 77 K. Dotted lines: Excitation and emission spectra of 4,4′-H_2bpy recorded at 77 K. The intensity values for all emission and excitation spectra were normalized.

(Figure 4). The relatively weak photoluminescence of compound **3** at room temperature becomes much stronger at 77 K. The extrapolation of the excitation band to zero intensity gives a band gap of 3.32 eV, which agrees (within the experimental error) with the value of 3.34 eV obtained using diffuse-reflectance measurements. 4,4′-bipy shows also photoluminescence at 440 nm (2.86 eV) when excited at 343 nm (3.62 eV) (Figure 4). Since the 4,4′-bipy molecules in **3** are protonated, we decided to examine also the photoluminescence properties of 4,4′-H_2bipyCl_2. With an excitation line of 3.74 eV (332 nm) intense green emission was observed at 77 K for 4,4′-H_2bipyCl_2 with a maximum at 2.43 eV (511 nm). In contrast, the discrete cluster compound **2** does not exhibit any photoluminescence. Thus, the blue-light emission of **3** may originate from the presence of the 4,4′-bpy molecules in this compound. However, both the cluster and 4,4′-bpy molecules are required for the observed photoluminescence of **3**, since (a) light emission was observed even with excitation energies below the $\pi-\pi'$ transition of bipyridine (3.62 and 3.74 eV for 4,4′-bpy and 4,4′-H_2bpyCl_2, respectively) and (b) there is a blue shift of the emission energy of **3** in relation to the emission energy of 4,4′-H_2bipyCl_2. This large energy difference between the excitation energies, as well as the emission ones, of compound **3** and 4,4′-bpy might be attributed to the strong interactions (hydrogen bonds) between the 4,4′-bipy groups and the cluster units in **3**. Since **3** is a 3D polymer and not a discrete molecular compound like for example compound **1**, the optical absorption of **3** is likely due to the excitation between electron bands rather than across molecular orbitals. *The blue photoluminescence indicates that **3** could be a good candidate for blue-light photoactive material.*

Theoretical Study. The wavenumbers of the fundamentals of the free sulfite dianion, according to the IR spectra of aqueous sulfite solutions,[36] are the following: $\nu_1(A_1) =$ 967 cm^{-1}; $\nu_2(A_1) = 620$ cm^{-1}; $\nu_3(E) = 933$ cm^{-1}; $\nu_4(E) =$ 469 cm^{-1}. ν_1 and ν_3 are stretching vibrations, whereas ν_2 and ν_4 are bending vibrations. Besides the expected shift of these bands upon coordination, the local symmetry of the sulfite ions in the four modes found in compound **4** (μ_2-*S,O*, μ_3-*S,O,O*, η^1-*O*, and η^1-*S*) is reduced from C_{3v} to near C_s resulting in the split of the E modes to A′ and A′ and giving rise to a variety of bands. The expected overlap between the Mo═O and SO stretches and Mo−O and SO bending complicated further the IR spectrum of the compound. To overcome the difficulty of the interpretation of the spectrum, we carried out density functional calculations for compound **4**. The experimentally observed μ_{eff} value showed that the compound is diamagnetic. Thus, the calculation has been done on the singlet state, whereas the calculated energy of an optimized structure with four unpaired electrons corresponding to a high-spin octahedral Co(III) configuration was very high. The optimized under the C_s symmetry constraints geometry of the compound in its singlet closed-

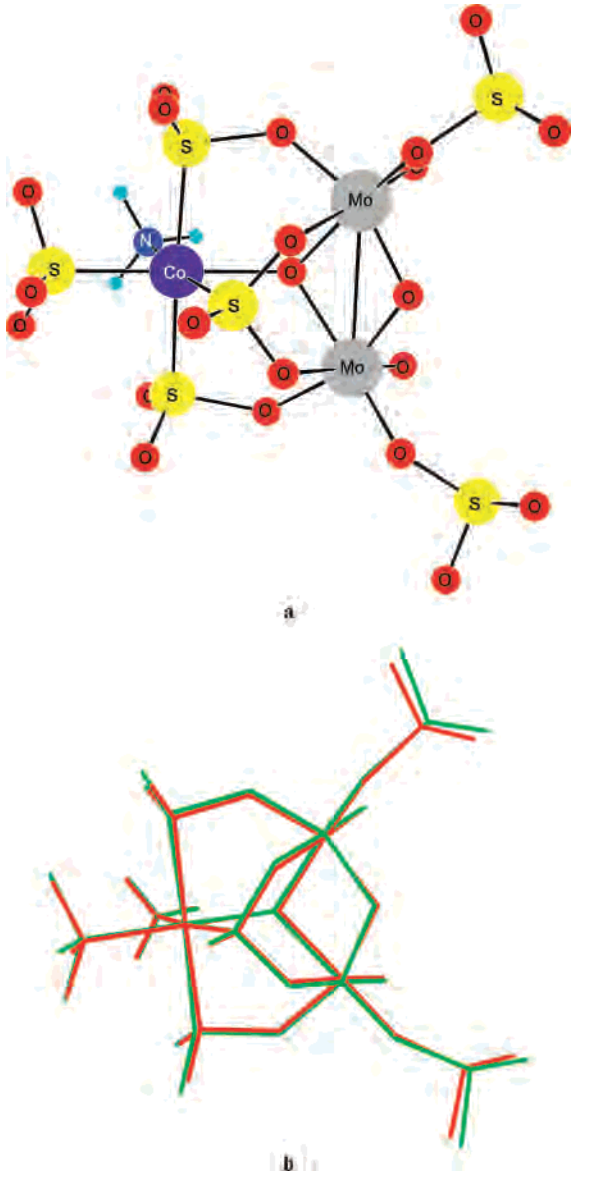

Figure 5. Optimized geometry of the anion of compound **4** (a) and overlay of its calculated (green) and experimental (red) structures (b).

(36) Nakamoto, P. K. *Infrared and Raman Spectra of Inorganic and Coordination Compounds*; Wiley: New York, 1986.

Table 3. Calculated and Experimental Bond Lengths (Å) for the Co(III) and Mo(V) Coordination Spheres for Compound **4**[a]

bond	calcd	expt (mean values)
Mo(1)−Mo(2)	2.635	2.585
Mo(1)−O(1)	1.705	1.688
Mo(1)−O(3)	1.913	1.948
Mo(1)−O(4)	2.049	1.953
Mo(1)−O(11)	2.312	2.351
Mo(1)−O(21)	1.995	2.092
Co(1)−O(4)	2.005	1.929
Co(1)−S(1)	2.249	2.222
Co(1)−S(2)	2.255	2.292
Co(1)−S(6)	2.238	2.206
Co(1)−N(1)	1.994	1.960

[a] Numbering scheme as in Figure 3.

Table 4. Calculated and Experimental Vibrational Frequencies (cm^{-1}) for Compound **4** in the Region 600−1200 cm^{-1} Along with Their Assignments

calcd	expt	assgnt
626	619 sh	η^1-*O*(SO_3^{2-}) bend, η^1-*S*(SO_3^{2-}) bend, Mo−O stretch
656	634 s	η^1-*O*(SO_3^{2-}) bend, Mo−O−Mo def
709	659 vs	η^1-*O*(SO_3^{2-}) bend, Mo−O stretch
794	752 s	μ_3-*S,O,O*(SO_3^{2-}) stretch, Mo−O stretch
810	858 m	μ_3-*S,O,O*(SO_3^{2-}) stretch
933	931 s	η^1-*S*(SO_3^{2-}) stretch
960	948 vs	Mo═O stretch
1004	968 s	η^1-*O*(SO_3^{2-}) stretch
1025	1009 sh	μ_2-*S,O*(SO_3^{2-}) stretch, μ_3-*S,O,O*(SO_3^{2-}) stretch
1038	1027 vs	μ_2-*S,O*(SO_3^{2-}) stretch, μ_3-*S,O,O*(SO_3^{2-}) stretch
1066	1056 s	η^1-*O*(SO_3^{2-}) stretch
1121	1074 sh	η^1-*S*(SO_3^{2-}) stretch
1138	1116 s	μ_2-*S,O*(SO_3^{2-}) stretch, μ_3-*S,O,O*(SO_3^{2-}) stretch, η^1-*S*(SO_3^{2-}) stretch
1161	1145 s	μ_2-*S,O*(SO_3^{2-}) stretch, μ_3-*S,O,O*(SO_3^{2-}) stretch

shell state is shown in Figure 5a, whereas the optimized bond lengths concerning the coordination spheres of Mo(V) and Co(III) are given in Table 3. There is an apparent overall agreement between the calculated geometry with this found experimentally, as it can be seen from the overlay of the calculated and experimental structures shown in Figure 5b. Calculation of the Hessian for the optimized structure gave the frequencies of the fundamental vibrations of the compound. The frequencies and description of the most intense of them in the region 600−1200 cm^{-1}, concerning the sulfite ion and Mo═O and M−O bonds, are given in Table 4, along with the corresponding experimental frequencies, whereas the experimental and simulated calculated spectra in the same region are shown in Figure S4. In low wavenumbers, the bands observed correspond to bending vibrations of the sulfite ions strongly mixed with Mo−O stretching (619 sh, 659 vs, 752 s) as well as deformation vibration of the Mo−O−Mo unit (634 s). Above 800 cm^{-1}, all bands correspond to stretching vibrations of the sulfite, except the 948 vs band which is assigned to Mo═O stretching. From them the 931 s, 968 s, 1056 s, and 1074 sh are located to the monodentate *S*-, or *O*-ligated sulfite ions, whereas the rest are stretching modes spread out to the bridged μ_2-*S,O* and, μ_3-*S,O,O* sulfite ligands.

Conclusion

In summary, a series of Mo^{VI}/SO_3^{2-}, Mo^{VI}/SO_3^{2-}-4,4′-H_2-$bipy^{2+}$, and $Mo^{V}/Co^{III}SO_3^{2-}$ compounds has been synthesized and structurally and physicochemically characterized. The directing influence of the solvent (H_2O/CH_3CN) was demonstrated by the isolation of compound **1** and not **2** (H_2O). The incorporation (through hydrogen bonding) of the protonated organic counterion, 4,4′-H_2bipy^{2+}, in the cluster, $[Mo_5^{VI}S_2O_{21}]^{4-}$, of compound **2** results in the isolation of a 3D polymer, compound **3**, which is a chiral, an NLO-active, and also a blue photoluminescent material. The latter property makes it a potential candidate as a blue-light photoactive material for practical applications. The organic molecule 4,4′-bipy has received a massive amount of attention as coordinative component for the synthesis of metal organic frameworks (MOF_5). This work provides a contrast, showing the importance of noncovalent oriented hydrogen-bonding interactions, which although relativey weak in comparison to a covalent bond can readily cause remarkable symmetry changes in the framework, thus pointing to effective ways of manipulating known materials or designing new materials with targeted properties. When cobalt(II) was introduced to the molybdenum(VI)/sulfite system an entirely new chemistry emerged with the isolation of the novel trinuclear mixed-metal [$Co^{III}-Mo_2^{V}-SO_3^{2-}$] species, **4**, which is the first mixed metal−sulfite cluster to date and augurs well that it is merely the prototype of a rich new area of mixed metal−sulfite heteropolyanion chemistry. Furthermore, the novel μ_4-η^2:η^2-O,*O* and μ_3-η^1:η^1:η^1-*O,O,S* modes of coordination of pyramidal sulfite anion in compounds **1** and **4**, respectively, reveal the great versatility of the sulfite anion to act as an excellent ligand in POMs and in the coordination compounds in general.

Acknowledgment. This research was cofunded by the European Union in the framework of the program "Pythagoras II" of the "Operational Program for Education and Initial Vocational Training" of the 3rd Community Support Framework of the Hellenic Ministry of Education, funded by 25% from national sources and by 75% from the European Social Fund (ESF). We thank the central laser facility of the University of Ioannina for the NLO measurements. We are grateful to the Ring of Laboratory Units and Centers of the University of Ioannina for the thermal analyses and Associate Professor T. Vaimakis for helpful discussions in thermal analysis. We also thank Prof. J. Pessoa for the elemental analyses and CD spectra as well as Mrs. F. Masala and Mrs. K. Statira for typing the manuscript and for fine English corrections, respectively.

Supporting Information Available: Additional tables and figures. This material is available free of charge via the Internet at http://pubs.acs.org.

IC700460B